A comparison of gravimetric geoid models over Western Australia, computed using modified forms of Stokes's integral

W E Featherstone

School of Spatial Sciences, Curtin University of Technology,

GPO Box U1987, Perth WA 6845

Abstract

Gravimetric models of the geoid over Western Australia have been constructed using two adapted forms of Stokes's integral; one uses the unmodified Stokes kernel with a global geopotential model and the other uses a deterministically modified kernel with a global geopotential model. The solutions use a combination of the complete expansion of the EGM96 global geopotential model with Australian gravity and terrain data. The resulting combined solutions for the geoid are compared with the control given by Global Positioning System (GPS) and Australian Height Datum heights at 63 points over Western Australia. The improved fit of the model that uses a modification to Stokes's kernel shows that this approach is more appropriate for gravimetric geoid computations over Western Australia.

1 Introduction

The geoid is the equipotential surface of the Earth's gravity field, which corresponds most closely with mean sea-level (ignoring oceanographic effects) and undulates with respect to an ellipsoidal model of the figure of the Earth. In 1849, G. G. Stokes published a solution to the boundary value problem of geodesy, which requires a global integration of gravity data over the Earth to compute the separation (N) between the geoid and reference ellipsoid

(Stokes, 1849). However, the incomplete global coverage and availability of accurate gravity measurements has precluded an exact determination of the geoid using Stokes's formula. Instead, an approximate solution is used in practice, where only gravity data in and around the computation area are used. This approach is also attractive because of the increase in computational efficiency that is offered by working with a smaller integration area.

In 1958, M. S. Molodensky (cited in Molodensky et al., 1962) proposed a modification to Stokes's formula to reduce the truncation error that results when gravity data are used over a limited area. However, Molodensky's modification did not receive a great deal of attention at that time because of the contemporaneous availability of low-frequency global gravity field information, derived from the analysis of the orbits of artificial Earth satellites. These global geopotential models are expressed in terms of fully normalised spherical harmonic functions and are now routinely used in conjunction with terrestrial gravity data via a truncated form of Stokes's integral (eg. Vincent and Marsh, 1973; Sideris and She, 1995). This combined approach reduces the truncation error because its series expansion begins at a higher degree, where the truncation coefficients are smaller in magnitude (assuming that the global geopotential model is an exact fit to the low-degree terrestrial gravity field). Another advantage of this combined solution for the geoid is that it reduces the impact of the spherical approximation inherent to the derivation of Stokes's integral (eg. Heiskanen and Moritz, 1967); the reason being that most of the geoid's power is contained in the low frequencies.

1.1 The generalised Stokes scheme

A formal representation of the combination of a global geopotential model with terrestrial gravity data has been proposed by Vaníček and Sjöberg (1991), which they refer to as the generalised Stokes scheme for geoid computation. Importantly, this satisfies a solution to the geodetic boundary value problem when formulated for a higher than second-degree reference model of the figure of the Earth (Martinec and Vaníček, 1997). In this scheme, the low-frequency geoid undulations generated by a global geopotential model (N_M) are extended

into the high frequencies by a global integration of complementary high-frequency, terrestrial gravity anomalies (Δg^M) using

$$N = N_M + \kappa \int_0^{2\pi} \int_0^{\pi} S^M(\cos \psi) \, \Delta g^M \, \sin \psi \, d\psi \, d\alpha \quad , \tag{1}$$

where $\kappa=R/4\pi\gamma$, R is the spherical Earth radius, γ is normal gravity evaluated on the surface of the geocentric reference ellipsoid as required by Bruns's formula (eg. Heiskanen and Moritz, 1967), ψ and α are the coordinates of spherical distance and azimuth angle about the computation point, respectively, and $S^M(\cos\psi)$ is the spheroidal form of Stokes's integration kernel, which is implicit to the generalised scheme and has the series expansion

$$S^{M}(\cos \psi) = \sum_{n=M+1}^{\infty} \frac{2n+1}{n-1} P_{n}(\cos \psi) , \qquad (2)$$

where $P_n(\cos \psi)$ is the *n*-th degree Legendre polynomial.

In Eq. (1), the low-frequency component of the geoid (N_M) is computed from the fully normalised spherical harmonic coefficients that define the global geopotential model according to

$$N_M = \frac{GM_e}{r\gamma} \sum_{n=2}^M \left(\frac{a}{r}\right)^n \sum_{m=0}^n (\delta \overline{C}_{nm} \cos m\lambda + \overline{S}_{nm} \sin m\lambda) \overline{P}_n^m(\cos \theta) . \tag{3}$$

The corresponding high-frequency gravity anomalies (Δg^M) are evaluated by subtracting the same spherical harmonic degrees of the same global geopotential model from the terrestrial gravity anomalies (Δg) according to

$$\Delta g^{M} = \Delta g - \frac{GM_e}{r^2} \sum_{n=2}^{M} \left(\frac{a}{r}\right)^n (n-1) \sum_{m=0}^{n} (\delta \overline{C}_{nm} \cos m\lambda + \overline{S}_{nm} \sin m\lambda) \overline{P}_n^m(\cos \theta) . \tag{4}$$

In Eqs. (3) and (4), GM_e is the product of the Newtonian gravitational constant and mass of the solid Earth, oceans and atmosphere, a is the equatorial radius of the reference ellipsoid, (r, θ, λ) are the geocentric spherical polar coordinates of each computation point, $\delta \overline{C}_{nm}$ and \overline{S}_{nm} are the fully normalised geopotential coefficients of degree n and order m, which have been reduced by the even zonal harmonics of the reference ellipsoid, and $\overline{P}_n^m(\cos \theta)$ are the fully normalised associated Legendre functions. It is assumed that the reference ellipsoid is

geocentric and has the same mass, potential and rotation rate as the geoid, such that the zero and first degree harmonics are inadmissible (eg. Heiskanen and Moritz, 1967).

The degree of spheroid (M) chosen for the generalised scheme can be driven by the maximum degree of global geopotential model available, which is usually $M_{max} = 360$. However, there are more important considerations than simply taking the maximum degree of expansion available (eg. Featherstone, 1992). Firstly, the $M_{max}=360$ models are already combined solutions for the geoid because they are constructed from both satellite-derived and terrestrial gravity data. Therefore, the same terrestrial gravity data are usually used twice in Eq. (1), which gives rise to unknown correlations between these data that are rarely accounted for or even acknowledged by some authors. Another consideration is the leakage of low-frequency errors from the terrestrial gravity data into the combined solution for the geoid, which can be filtered by the spheroidal kernel due to the orthogonality of spherical harmonic functions over the sphere (eg. Vaníček and Featherstone, 1998). This is considered to be a desirable scenario because the low-frequency geopotential coefficients are currently the best source of this information, whereas terrestrial gravity data are subject to low-frequency errors. Therefore, choosing the degree of spheroid at say M=20 in Eq. (1), which is the limit of the reliable resolution of the satellite-derived geopotential coefficients, both avoids the correlations and reduces the leakage of terrestrial gravity anomaly errors.

2 Reductions of the Approximation Error

2.1 The generalised Stokes scheme

The generalised Stokes scheme (Eq. 1) remains subject to a truncation error when high-frequency terrestrial gravity anomalies are used over a limited area. Accordingly, there is an adjustment of Eq. (1) that involves limiting the integration domain to a spherical cap of radius ψ_0 ($0 \le \psi_0 \le \pi$) about each geoid computation point, which yields the approximation

$$\hat{N}_1 \simeq N_M + \kappa \int_0^{2\pi} \int_0^{\psi_0} S^M(\cos \psi) \, \Delta g^M \, \sin \psi \, d\psi \, d\alpha \tag{5}$$

with a corresponding truncation error of

$$\delta N_1 = \kappa \int_0^{2\pi} \int_{\psi_0}^{\pi} S^M(\cos \psi) \, \Delta g^M \, \sin \psi \, d\psi \, d\alpha \, , \tag{6}$$

such that $N = \hat{N}_1 + \delta N_1$. This truncation error can be expressed as a series expansion by

$$\delta N_1 = 2\pi\kappa \sum_{n=M+1}^{\infty} Q_n^M(\psi_o) \,\Delta g_n \quad , \tag{7}$$

where the spheroidal truncation coefficients

$$Q_n^M(\psi_o) = \int_{\psi_o}^{\pi} S^M(\cos \psi) P_n(\cos \psi) \sin \psi \, d\psi \tag{8}$$

can be evaluated using the algorithms of Paul (1973). The n-th degree surface spherical harmonic of the gravity anomaly

$$\Delta g_n = \frac{GM}{r^2} \left(\frac{a}{r}\right)^n (n-1) \sum_{m=0}^n (\delta \overline{C}_{nm} \cos m\lambda + \overline{S}_{nm} \sin m\lambda) \overline{P}_n^m(\cos \theta)$$
(9)

can be evaluated for each n upto the maximum degree (M_{max}) of the geopotential model. As such, the truncation error in Eq. (7) reduces to

$$\delta N_1 = 2\pi\kappa \sum_{n=M_{max}+1}^{\infty} Q_n^M(\psi_o) \, \Delta g_n \tag{10}$$

However, if $\Delta g^M \neq 0$ ($2 \leq n \leq M$), which is true if the global geopotential model is not an exact fit to the low-frequency terrestrial gravity field, there is a leakage of any low-frequency gravity errors into the low-frequency geoid solution when the integration is performed over a limited area (Vaníček and Featherstone, 1998). This is a direct consequence of the approximation of the generalised Stokes integral (Eq. 5), which introduces the non-zero truncation coefficients in the region $2 \leq n \leq M$ because the orthogonality of spherical harmonics breaks down under the approximation in Eq. (5). Since Δg_n only depend on the physical properties of the Earth, it becomes necessary to seek a modification to the integration kernel that reduces the magnitude of the truncation coefficients and hence the truncation error. Ideally, this modification should reduce the truncation error as well as making the kernel behave as a (partial) high-pass filter so as to reduce the leakage of any low-frequency terrestrial gravity data errors (Vaníček and Featherstone, 1998).

2.2 The remove-compute-restore scheme

The remove-compute-restore technique (eg. Torge, 1991) has almost become a standard approach in regional combined solutions for the geoid. However, most users of this approach make no attempt to modify the integration kernel and thus reduce the truncation error or adapt its filtering properties. Instead, this scheme uses the unmodified kernel as originally introduced by Stokes (eg. Sideris and She, 1995; Smith and Milbert, 1999). The remove-compute-restore approach also generally uses the maximum degree of the global geopotential model (M_{max}) , which gives rise to the data combination

$$\hat{N}_2 \simeq N_{M_{max}} + \kappa \int_0^{2\pi} \int_0^{\psi_0} S(\cos\psi) \, \Delta g^{M_{max}} \, \sin\psi \, d\psi \, d\alpha \tag{11}$$

where the terms $N_{M_{max}}$ and $\Delta g^{M_{max}}$ are computed from the maximum available degree and order of a global geopotential model (Eqs. 3 and 4), and the unmodified Stokes kernel is given by

$$S(\cos\psi) = \sum_{n=2}^{\infty} \frac{2n+1}{n-1} P_n(\cos\psi)$$
(12)

In this combined solution for the geoid, the truncation error has to be neglected because it cannot be computed since the complete expansion of the global geopotential model has already been used. This also makes it subject to the correlation of errors between the global geopotential model and terrestrial gravity data used in the regional geoid solution. Moreover, no other attempt has been made to reduce the truncation error or adapt the filtering properties of the integration kernel. Admittedly, the truncation error will reduced a great deal if the global geopotential model is a good fit to the terrestrial gravity anomalies in the area of interest (ie. if $\Delta g^M = 0$ in the region $2 \le n \le M_{max}$). However, the penalty of taking this approach is that any errors in the terrestrial gravity anomalies to propagate unattenuated into the combined solution for the geoid (eg. Vaníček and Featherstone, 1998). It must also be acknowledged that, despite these restrictions, the remove-compute-restore technique has delivered quite reasonable results (eg. Sideris and She, 1995; Smith and Milbert, 1999). However, the question of whether a modified integration kernel in the generalised

Stokes scheme will deliver even better results remains, and thus forms the primary aim of this investigation.

2.3 Integration kernel modifications

As argued above, it remains preferable to apply a modification to the approximated form of the generalised Stokes's integral (Eq. 5) so as to further reduce the associated truncation error. Since Molodensky's pioneering work, several other authors have proposed modifications to Stokes's (1849) integral. These have been based on different criteria and can be broadly classified as deterministic modifications (eg. Molodensky et al., 1962; Wong and Gore, 1969; Meissl, 1971; Heck and Grüninger, 1987; Vaníček and Kleusberg, 1987; Vaníček and Sjöberg, 1991; Featherstone et al., 1998) and stochastic modifications (eg. Wenzel, 1982; Sjöberg, 1991; Vaníček and Sjöberg, 1991). The stochastic modifications, whilst offering an optimal combination of the two data types together with a minimisation of the truncation error (in a least-squares sense), require reliable variance estimates of the data. However, the error characteristics of the terrestrial gravity data over Western Australia and over most other parts of the world are currently unknown, which renders the stochastic modifications of limited practical use. Therefore, the deterministic kernel modifications will have to be relied upon in the interim.

The deterministic kernel modifications can be further divided into two broad categories: modifications that reduce the upper bound of the truncation error according to some prescribed norm, and modifications that improve the rate of convergence of the series expansion of the truncation error. The modification proposed by Featherstone *et al.* (1998) uses a combination of these, where the rate of convergence of the series expansion of an already-reduced truncation error by the L_2 norm (Vaníček and Kleusberg, 1987) is accelerated from $O(n^{-1})$ to $O(n^{-2})$ through the approach proposed by Meissl (1971). This can be achieved either by setting the kernel to zero at the truncation radius through subtraction, or by choosing the truncation radius such that it coincides with a zero point of the kernel.

The Featherstone et al. (1998) modification is given by

$$S_L^M(\cos\psi) = S^M(\cos\psi) - S^M(\cos\psi_0) - \sum_{k=2}^L \frac{2k+1}{2} t_k(\psi_0) \left[P_k(\cos\psi) - P_k(\cos\psi_0) \right] , \quad (13)$$

where the $t_k(\psi_0)$ modification coefficients are computed from the solution of the following set of L-1 linear equations, once the truncation radius (ψ_0) has been chosen

$$\sum_{k=2}^{L} \frac{2k+1}{2} t_k(\psi_0) e_{nk}(\psi_0) = Q_n^M(\psi_0) , \qquad (14)$$

where

$$e_{nk}(\psi_0) = \int_{\psi_0}^{\pi} P_n(\cos\psi) P_k(\cos\psi) \sin\psi \, d\psi \quad , \tag{15}$$

which can be evaluated using the recursive algorithms of Paul (1973). The degree of this kernel modification (L) can be chosen to be greater than, equal to or less than the degree of the spheroid (M) embedded in the generalised Stokes formula (Eq. 1). If L > M, additional terms arise due to this disparate combination and should be computed or their omission acknowledged.

2.4 A compromise of the combined solution

The combined solution for the geoid considered in this study attempts to reach a compromise of the above two schemes, based on considerations of the data availability, their expected reliability and a reduction of the truncation error through the above deterministic modification of the generalised Stokes kernel. This compromise approach was used to compute the recent Australian gravimetric geoid model AUSGeoid98 (Johnston and Featherstone, 1998). Mathematically, this is formalised as

$$\hat{N}_3 \simeq N_{M_{max}} + \kappa \int_0^{2\pi} \int_0^{\psi_0} S_L^M(\cos\psi) \, \Delta g^{M_{max}} \, \sin\psi \, d\psi \, d\alpha \quad , \tag{16}$$

where all terms are as defined earlier.

Equation (16) utilises the maximum available expansion (M_{max}) of the global geopotential model in conjunction with a low-degree (L) of deterministic kernel modification. This approach aims at reducing the truncation error so that it can be safely ignored, whilst relying

more on the low-degree satellite solution by filtering a proportion of the low-frequency errors from the terrestrial gravity data (cf. Vaníček and Featherstone, 1998). However, this choice is also driven by some practical considerations. Empirical studies by Featherstone (1992) indicate that the modified kernels become numerically unstable for large L and small ψ_0 , which enforces a low degree of kernel modification when a small integration radius is used. For simplicity, the degree of kernel modification is chosen equal to the degree of spheroid used in the generalised scheme (ie. L = M = 20). The integration radius was chosen to be $\psi_0 = 1^{\circ}$, since this value was empirically selected for AUSGeoid98 (Johnston and Featherstone, 1998).

It is argued that this offers a geoid solution that is superior to the application of the remove-compute-restore technique with an unmodified kernel because of its further reduction of the truncation error and adaption of the filtering properties of the kernel. However, it is also important to acknowledge the deficiencies of this attempted compromise, which are the use of the high-frequencies in the global geopotential model (which can contain 80% noise; eg. Lemoine et al., 1998) and the correlations between the terrestrial gravity data in the region $20 < n \le M_{max}$. Therefore, empirical tests are used in Western Australia to determine whether the use of a deterministically modified integration kernel is more appropriate than using the unmodified kernel.

3 Empirical tests in Western Australia

The tests that follow compare the combined solutions for the geoid, computed using Eqs. (11) and (16), with discrete geoid heights at 63 points across Western Australia. These control data are derived from Global Positioning System (GPS) measurements at Australian Height Datum (AHD) benchmarks. The difference between a GPS-derived ellipsoidal height and geodetically levelled height with respect to mean sea level gives a discrete estimate of the separation between the geoid and reference ellipsoid. Assuming that there are no errors in these control data, the gravimetric geoid solution that delivers the best fit can be considered

to be the most suitable for Western Australia.

3.1 Data and its processing

The EGM96 global geopotential model (Lemoine et al., 1998), complete to $M_{max} = 360$, was used in this study. EGM96 is one of the most recent global geopotential models and was produced by the US National Imagery and Mapping Authority (NIMA) — formerly the Defense Mapping Agency (DMA) — and the US National Aeronautical and Space Administration's (NASA) Goddard Space Flight Center (GSFC). Kirby et al. (1998) compared EGM96 with Australian gravity data (described below) and discrete geoid heights provided by co-located GPS and AHD data. This showed that EGM96 proved a slightly better (though statistically not significant) representation of the Australian gravity field than its predecessors.

The Australian Geological Survey Organisation's (AGSO) 1996 national gravity data release, being the most recent available to the author, has been used in the computations. As most of the AGSO gravity data were collected and reduced predominantly for geophysical exploration purposes, they are not necessarily suited to the requirements of gravimetric geoid computation. As such, they have been validated according to the procedures in Featherstone et al. (1997) and the gravity anomalies computed using the more stringent geodetic approaches (eg. Featherstone, 1995). Deficiencies were also found in the mean free-air gravity anomalies computed on land, due to the gravity data collection strategies used by AGSO. The land gravity observations were typically made along roads and tracks in areas of rugged terrain, which usually follow valleys or areas of least height variation. A similar, though opposite, effect occurs in central Australia where most observations were performed using helicopter transport. These observations were often located on raised ground where convenient landing spots were identified. Specifically, the computed mean gravity anomaly does not truly represent the actual mean gravity anomaly of an area. As such, the resultant geoid are biased by these observation techniques. To numerically counter this biasing effect, a digital elevation model (described below), which gives a better representation of the mean height than the gravity observation elevations, was used to reconstruct more representative mean gravity anomalies (Featherstone and Kirby, 1999).

Satellite-altimeter-derived marine gravity anomalies were used offshore Australia to supplement AGSO's marine gravity data coverage. These gravity anomalies were computed from a combination of satellite-borne radar altimeter missions and supplied on a 2' by 2' grid (Sandwell and Smith, 1997). These data significantly improve the gravity data coverage offshore Australia and, as such, were expected to give an improved geoid solution in marine areas and on land areas close to the coast. However, errors thought to reside in the lowfrequency altimeter-derived gravity anomalies adversely affect the gravimetric geoid near the coast, which was indicated by comparisons of the geoid solution with GPS and AHD data near the coast. The low-frequency errors in the satellite altimeter data are probably due to a combination of un-modelled near-shore sea-surface topography and backscatter of altimeter returns from the land. Another explanation for this observed deficiency comes from the conversion of sea surface heights, which are the direct measurements taken by the altimeter, to gravity anomalies, then converting these gravity anomalies to geoid heights. At present, it is unknown how the errors, such as un-modelled sea-surface topography, propagate through the approximations used in these processes. Therefore, as an interim and practical solution, least squares collocation (eg. Moritz, 1980b) was used to 'drape' the altimeter gravity anomalies onto the AGSO marine gravity anomalies (Kirby and Forsberg, 1998). This approach then improved the geoid solution near the coast, when compared with GPS and AHD data, over that achieved using only the AGSO marine gravity data or simple averaging of the AGSO marine gravity data and the satellite-altimeter data.

Gravimetric terrain corrections, based on the national 9" by 9" digital elevation model (Carrol and Morse, 1996), were evaluated using Moritz's (1968) formula via the fast Fourier transform or FFT (Kirby and Featherstone, 1999). The FFT offers the only practical way to compute detailed terrain corrections on a continental scale, since prism integration at this scale could take several months to evaluate. It was found (*ibid.*) that the terrain

correction computations had to be performed using a 27" by 27" grid to avoid the instability in Moritz's terrain correction algorithm that occurs for high-resolution digital terrain models close to the computation point (cf. Martinec et al., 1996). Associated with the gravimetric terrain correction are the primary and secondary indirect effects (eg. Wichiencharoen, 1982). The primary indirect effect accounts for the change in potential caused by the free-air gravity reduction and gravimetric terrain correction. The primary indirect effect was computed using the FFT on a 27" grid, which avoids the kernel instability and, moreover, is consistent with the terrain correction computations. The secondary indirect effect on gravity was computed by applying the free-air reduction over the geoid-compensated-geoid separation computed via the primary indirect effect. This resulted in an additional gravity term that was added to the gravity anomalies prior to geoid computation.

A grid of residual Faye gravity anomalies was computed from the AGSO gravity observations using the continuous curvature spline in tension algorithm (Smith and Wessel, 1990; Wessel and Smith, 1995). Residual Faye gravity anomalies are terrain-corrected free-air gravity anomalies that have been reduced by the gravity anomalies implied by the complete expansion of EGM96 (Eq. 4). A regular grid of residual Faye gravity anomalies is required for the residual geoid computations via the one-dimensional FFT technique. It is acknowledged that other gravity gridding techniques do exist, such as least squares collocation (Moritz, 1980b), but the continuous curvature spline in tension algorithm was readily available (Wessel and Smith, 1995) and gives similar results in a considerably shorter computation time (Zhang, 1998). For this study, a 2' by 2' grid of gravity anomalies was generated over the region $-11^{\circ} \le \phi \le -37^{\circ}$ and $110^{\circ} \le \lambda \le 131^{\circ}$, which covers the state of Western Australia. Table 1 summarises the statistical properties of the Faye gravity anomalies and the residual Faye gravity anomalies, where the $M_{max}=360$ expansion of EGM96 has been subtracted via Eq. (4). The GRS80 reference ellipsoid (Moritz, 1980a) has been used in all computations. Grey-scale images of the EGM96 gravity anomalies and residual Faye gravity anomalies are shown in Figures 1 and 2, respectively.

	max.	min.	mean	st. dev.	rms
Faye gravity anomalies	131.085	-147.678	-8.762	± 29.110	±30.400
residual Faye gravity anomalies	91.554	-101.236	0.009	± 10.968	± 10.968

Table 1. Statistical properties of the gravity anomalies over Western Australia (units in mGal).

The statistical fit of the gravity anomalies implied by the EGM96 global geopotential model to the gravity field of Western Australia is poorer than that experienced in other parts of the world (cf. Forsberg and Featherstone, 1998). This is probably due to the larger uncertainty in the computed gravity anomalies, which is principally caused by errors in the gravity station elevations (eg. Featherstone et al., 1997). However, since a large proportion of these data have been used in the construction of the EGM96 global geopotential model, a more likely explanation is an inaccuracy in the mean gravity anomalies used. Lemoine et al. (1998) describe the construction of the JGP95E 5' by 5' digital elevation model, where the Australian 5' by 5' digital elevation model was used west of $\lambda=136^{\circ}$ and a National Imagery and Mapping Agency (NIMA) digital elevation model was used east of $\lambda = 136^{\circ}$. The Australian 5' by 5' digital elevation model used was probably that constructed at the Australian National University from the elevations associated with the gravity station elevations. Featherstone and Kirby (1999) show that this digital elevation model is biased because the gravity observations do not accurately represent the topographic morphology (see earlier discussion). Therefore, more reliance should be placed on the terrestrial gravity anomalies described earlier, hence the use of a low-degree kernel modification.

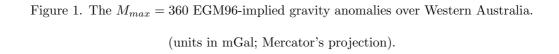


Figure 2. The residual Faye gravity anomalies over Western Australia. $(\hbox{units in mGal; Mercator's projection}).$

3.2 Geoid computation by the 1D-FFT technique

In the mid 1980s, the fast Fourier transform (FFT) technique began to find wide-spread use in gravimetric geoid computation, because of its efficient evaluation of convolution integrals when compared to quadrature-based numerical integration. For many years, the planar, two-dimensional FFT was used (eg. Schwarz et al., 1990). Strang van Hees (1990) then introduced the spherical, two-dimensional FFT. However, both of these FFT approaches are subject to approximation errors, the most notable of which is the simplification of Stokes's kernel. Forsberg and Sideris (1993) therefore proposed the spherical, multi-band FFT, which reduces the impact of the simplified kernel. Haagmans et al. (1993) then refined this approach to give the spherical, one-dimensional FFT, which requires no simplification of Stokes's kernel. For this reason, the 1D-FFT has been used in this investigation so that the exact kernels in Eqs. (12) and (13) can be used efficiently and without the need for a kernel simplification.

Another consideration is that remove-compute-restore determinations of the geoid using the 1D-FFT often convolve the whole rectangular grid of gravity anomalies over a region with the spherical Stokes kernel (eg. Sideris and She, 1995; Smith and Milbert, 1999). On the other hand, quadrature-based geoid determinations use only gravity anomalies over a spherical integration radius about each computation point. Therefore, each approach results in a different truncation error due to the neglect of the residual gravity anomalies in the (different shaped) remote zones outside each integration domain. Both of these implementations are tested in this study, where in Eq. (11) the spherical integration radius is set to $\psi_0 = \pi$ so as to use the whole gravity data rectangle, and $\psi_0 < \pi$ is used to mimic quadrature-based numerical integration.

In order to make the 1D-FFT approach closely mimic quadrature-based numerical integration over a spherical cap, the integration kernel is set to zero outside the truncation radius $(\psi_0 = 1^{\circ})$ before transformation to the frequency domain. A further adaption of this technique has been added to allow the 1D-FFT-based evaluation of Eq. (16), where the modified kernel (Eq. 13) was implemented by evaluating it before transformation to the frequency

domain (Featherstone and Sideris, 1998). Comparisons with quadrature-based numerical integration software that uses spherical caps and deterministically modified integration kernels (Featherstone, 1992) were used to verify these adaptions of the 1D-FFT.

In what follows, the gravimetric geoid heights from each approach have been evaluated using the 1D-FFT for (i) the remove-compute-restore technique with an unmodified kernel and residual Faye gravity anomalies over whole data area $\psi_0 = \pi$, (ii) the remove-compute-restore technique with an unmodified kernel and residual Faye gravity anomalies over a spherical cap of radius ($\psi_0 = 1^{\circ}$), and (iii) the compromise approach in Eq. (16) with a deterministically modified kernel and residual Faye gravity anomalies over a spherical cap ($\psi_0 = 1^{\circ}$). In the latter case, the degree of spheroid associated with the generalised Stokes scheme is M = 20 and the degree of deterministic kernel modification is the same (ie. L = 20). Of course, a large number of permutations of these parameters is possible by varying the degree of global geopotential model (M), integration radius (ψ_0), degree of kernel modification (L) and indeed the type of kernel modification (see Section 2.3). However, only these three cases are studied for Western Australia because the remove-compute-restore technique is used in many other parts of the world (eg. Sideris and She, 1995; Smith and Milbert, 1999), and the L = M = 20 modification for a cap radius of $\psi_0 = 1^{\circ}$ was used for AUSGeoid98 (Johnston and Featherstone, 1998).

All geoid computations were conducted on a 2' by 2' grid over an area bound by $-12^{\circ} \le \phi \le -36^{\circ}$ and $112^{\circ} \le \lambda \le 129^{\circ}$, which accounts for the edge effect associated with the one-degree integration radius (with the exception of the integration over the whole data area). It should be pointed out that this edge effect affects the whole computation area when the cap-radius is unlimited. Nevertheless, the comparisons are conducted over the same area.

3.3 Comparison of Geoid Results with GPS at AHD Benchmarks

As is customary in almost all validations of gravimetric geoid models on land (eg. Featherstone and Alexander, 1996), the geoid results from this study were compared with Global

Positioning System (GPS) and geodetic levelling data to determine if any improvements are made when utilising limited spherical integration caps and a deterministically modified kernel. However, it must be pointed out this type of comparison is inevitably biased because the geodetic levelling data used in this investigation are based on the Australian Height Datum (AHD), which is a normal orthometric height system based on estimates of mean sea level from 30 tide gauges around Australia (Roelse et al., 1971). As such, it does not give an exact representation of the equipotential geoid (eg. Featherstone, 1998). Nevertheless, GPS and geodetic levelling data currently provide the only (partially) independent means with which to verify a gravimetric geoid model on land. However, given that the primary geodetic application of a gravimetric geoid model is to transform GPS-derived ellipsoidal heights to the AHD, this type of analysis is useful to ascertain the gravimetric geoid models' performance for this application.

For each of the three cases investigated, the gravimetric geoid solution was bi-cubically interpolated from the 2' by 2' grid and statistically compared with 63 discrete geoid heights derived from the most precise GPS networks available in Western Australia (Morgan *et al.*, 1996; Stewart *et al.*, 1997) for points that are co-located with geodetically levelled heights of third order, or better, on the AHD. Table 2 shows a statistical summary of the differences between the 63 control geoid heights and the results from EGM96 alone (Eq. 3), the 1D-FFT implementations of Eq. (11) with $\psi_0 = \pi$ and $\psi_0 = 1^\circ$, and Eq. (16) with $\psi_0 = 1^\circ$. The mean differences in Table 2 should not be relied upon to choose the most accurate geoid solution because any gravimetric determination of the geoid is deficient in scale (ie. only the gravimetric geoid's precision can be estimated). This scale deficiency due to the imperfect knowledge of the mass of the Earth (cf. the text immediately after Eqs. (3) and (4)). Accordingly, only the standard deviations (st. dev.) of the fit of each gravimetric geoid model to the control data should be used to assess the performance in terms of precision of each model; the mean and root mean square (rms) values are only included for the sake of completeness.

The difference between the fit of each good model in Table 2 is not always significant in

	max.	min.	mean	st. dev.	rms
EGM96 only (Eq. 3)	0.889	-0.328	0.148	± 0.274	± 0.311
Eq. (11) with $\psi_0 = \pi$ and $S(\cos \psi)$	0.751	-0.776	-0.092	± 0.362	± 0.374
Eq. (11) with $\psi_0=1^\circ$ and $S(\cos\psi)$	0.625	-0.664	0.118	± 0.249	± 0.276
Eq. (16) with $\psi_0 = 1^{\circ}$ and $S_{20}^{20}(\cos \psi)$	0.761	-0.308	0.140	± 0.223	± 0.263

Table 2. The statistics of the absolute between the 63 control GPS-AHD heights and the gravimetric geoid heights computed from EGM96 only, Eq. (11) with $\psi_0=\pi$ and $\psi_0=1^\circ$, and Eq. (16) with $\psi_0=1^\circ$. (units in metres).

a statistical sense, when considering that the random error budget of the GPS data is 0.05m (Morgan et al., 1996; Stewart et al., 1997) and distortions of the AHD from the geoid are of the order of 1m (Roelse et al., 1971; Featherstone and Stewart, 1998). Despite these caveats, however, some useful inferences can be made from these results as follows.

Firstly, the use of the whole gravity data area in the combined solution for the geoid (Eq. 11 with $\psi_0=\pi$) gives a result that is worse than using the EGM96 global geopotential model alone (Table 2). Whilst the use of the whole data area appears to be appropriate in other parts of the world (eg. Sideris and She, 1995; Smith and Milbert, 1999), a considerably worse result is achieved in Australia when using this approach (Table 2; Forsberg and Featherstone, 1998; Johnston and Featherstone, 1998). This is a slightly unexpected result since, the more data that are included in the geoid solution should yield a better result. This is either due to noise in the Australian gravity anomalies, which been estimated to be approximately 2 mGal (Featherstone *et al.*, 1997), or the theoretical basis of this approach is unsuitable for Australia.

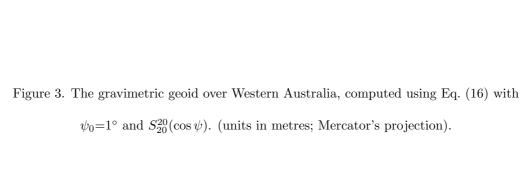
Next from Table 2, there is an improvement over the results of using only the EGM96 global geopotential model offered by the use of a limited integration radius in Eqs. (11). Importantly, there is a further improvement offered by using the deterministically modified

integration kernel in Eq. (16) for the same integration radius. Though inconclusive due to the perceived uncertainties in the control data, these results do indicate that the use of deterministically modified integration kernel is a preferable approach for geoid computations in Western Australia. Figure 3 shows a contour map of the gravimetric geoid model of Western Australia that has been computed using Eq. (16) with $\psi_0=1^{\circ}$ and $S_{20}^{20}(\cos\psi)$.

Finally, as the improvements offered by using a one-degree integration radius ($\psi_0=1^\circ$ in Eqs. 11 and 16) are not significantly better than using the EGM96 model alone. This suggests that the EGM96 global geopotential model provides most of the power in the combined solution for the geoid and thus dominates its performance. Given the earlier arguments that EGM96 may not offer the optimal model for Australia, this suggests that further work is required to determine the optimal selection of the degree of global geopotential model (M) as well as the optimal degree of kernel modification (L).

4 Conclusions

From these gravimetric geoid results over Western Australia, it is clear that 1D-FFT geoid computations should use a spherical cap of limited extent instead of the whole gravity data grid. Also, small though not necessarily statistically significant improvements are observed when a deterministically modified integration kernel is used over a spherical cap. This is because the kernel modification reduces the truncation error so that its neglect has less impact on the solution and adapts the filtering properties of the kernel. Therefore, it is recommended that limited integration caps and modified kernels are used in future spectral geoid determinations of Western Australia.



Acknowledgments

I would like to thank the Western Australian Department of Land Administration, the Australian Surveying and Land Information Group, the Australian Geological Survey Organisation, the US National Imagery and Mapping Authority, and the US National Aeronautics and Space Administration for providing data.

References

Caroll D, Morse MP 1996 A national digital elevation model for resource and environmental management, Cartography, 25(2): 395-405.

Featherstone WE 1992 A GPS controlled gravimetric determination of the geoid of the British Isles. D.Phil thesis, Oxford University, England.

Featherstone WE 1995 On the use of Australian geodetic datums in gravity field determination.

Geomatics Research Australasia, 62:17-37.

Featherstone WE, Alexander K 1996 An analysis of GPS height determination in Western Australia. The Australian Surveyor, 41(1):29-34.

Featherstone WE, Kearsley AHW, Gilliland JR 1997 Data preparations for a new Australian gravimetric geoid. The Australian Surveyor 42(1):33-44.

Featherstone WE, Stewart MP 1998 Possible evidence for distortions in the Australian Height Datum in Western Australia, Geomatics Research Australasia, 69: 1-14.

Featherstone WE, Sideris MG 1998 Modified kernels in spectral geoid determination: first results from Western Australia, in: Geodesy on the Move, Springer, Berlin.

Featherstone WE, Evans JD, Olliver JG 1998 A Meissl-modified Vaníček and Kleusberg kernel to reduce the truncation error in gravimetric geoid computations. Journal of Geodesy 72(3):154-160.

Featherstone WE 1998 Do we need a gravimetric geoid or a model of the base of the Australian Height Datum to transform GPS heights? The Australian Surveyor 43(4):273-280.

Featherstone WE, Kirby JF 1999 The reduction of aliasing in gravity observations using digital terrain data and its effect upon geoid computation, Geophysical Journal International, (submitted).

Forsberg R, Sideris MG 1993 Geoid computations by the multi-band spherical FFT approach.

Bulletin Géodésique 18:82-90.

Forsberg R, Featherstone WE 1998 Geoids and cap sizes. in: Geodesy on the Move, Springer, Berlin.

Heck B, Grüninger W 1987 Modification of Stokes's integral formula by combining two classical approaches. IUGG General Assembly, Vancouver, Canada.

Haagmans RR, de Min E, van Gelderen M 1993 Fast evaluation of convolution integrals on the sphere using 1D-FFT, and a comparison with existing methods for Stokes's integral. manuscripta geodaetica 18(5):227-241.

Heiskanen WH, Moritz H 1967 Physical Geodesy. WH Freeman and Co., San Francisco, USA. Johnston GM, Featherstone WE 1998 AUSGEOID98 computation and validation: exposing the hidden dimension, proceedings of the 39th Australian Surveyors Congress, Launceston, 105-116.

Kirby JF, Featherstone WE, Kearsley AHW 1998 Tests of the DMA/GSFC geopotential models over Australia. International Geoid Service Bulletin, 7: 1-14.

Kirby JF, Featherstone WE 1999 Terrain correcting the Australian gravity data base using the national digital elevation model and the fast Fourier transform, Australian Journal of Earth Sciences, (in press).

Kirby JF, Forsberg R 1998 A comparison of techniques for the integration of satellite altimeter and surface gravity data for geoid determination. in: Gravity and Geoids, Springer, Berlin. Lemoine FG, Kenyon SC, Factor JK, Trimmer RG, Pavlis NK, Chinn DS, Cox CM, Klosko SM, Luthcke SB, Torrence MH, Wang YM, Williamson RG, Pavlis EC, Rapp RH, Olson TR 1998 The development of the joint NASA GSFC and the National Imagery and Mapping Agency (NIMA) geopotential model EGM96, NASA/TP-1998-206861, National Aeronautics

and Space Administration, Maryland, USA.

Martinec Z, Vaníček P, Mainville A, Véronneau M 1996 Evaluation of topographical effects in precise geoid computation from densely sampled heights. Journal of Geodesy, 70(11): 746-754.

Martinec Z, Vaníček P 1997 Formulation of the boundary-value problem for geoid determination with a higher-degree reference field. Geophysical Journal International, 126(1): 219-228.

Meissl P 1971 Preparations for the numerical evaluation of second-order Molodensky-type formulas. OSU Report 163, Department of Geodetic Science and Surveying, Ohio State University, Columbus, USA.

Molodensky MS, Eremeev VF, Yurkina MI 1962 Methods for Study of the External Gravitational Field and Figure of the Earth. Israeli Programme for the Translation of Scientific Publications, Jerusalem, Israel.

Morgan P, Bock Y, Coleman R, Feng P, Garrard D, Johnston G, Luton G, McDowall B, Pearse M, Rizos C, Tiesler R 1996 A zero-order GPS network for the Australian region.

Report ISE-TR 96/60, University of Canberra, Canberra, Australia.

Moritz H 1968 On the use of the terrain correction in solving Molodensky's problem, Report 108, Department of Geodetic Science and Surveying, Ohio State University, USA.

Moritz H 1980a Geodetic Reference System 1980, Bulletin Géodésique, 54(4):395-405.

Moritz H 1980b Advanced Physical Geodesy, Wichmann, Karlsruhe.

Paul MK 1973 A method of evaluating the truncation error coefficients for geoidal height, Bulletin Géodésique 47:413-425.

Roelse A, Granger HW, Graham JW 1971 The adjustment of the Australian levelling survey - 1970-71. Report 12, National Mapping Council of Australia, Canberra.

Sandwell DT, Smith WHF 1997 Marine gravity anomaly from Geosat and ERS 1 satellite altimetry, Journal of Geophysical Research, 102(B5):10039-10054

Schwarz KP, Sideris MG, Forsberg R 1990 The use of FFT techniques in physical geodesy. Geophysical Journal International 100:485-514.

Sideris MG, She BB 1995 A new, high-resolution geoid for Canada and part of the US by the 1D-FFT method. Bulletin Géodésique, 69(2):92-108.

Sjöberg LE 1991 Refined least squares modification of Stokes's formula. manuscripta geodaetica 16:367-375.

Smith D, Milbert DG 1999 A gravimetric geoid of the United States. Journal of Geodesy (in press).

Smith WHF, Wessel P 1990 Gridding with continuous curvature splines in tension, Geophysics 55(3):293-305.

Stewart MP, Ding X, Tsakiri M, Featherstone WE 1997 The 1996 STATEFIX Project Final Report. Contract Report, School of Surveying and Land Information, Curtin U niversity of Technology, Perth, Australia.

Stokes GG 1849 On the variation of gravity on the surface of the Earth. Transactions of the Cambridge Philosophical Society 8:672-695.

Strang van Hees GL 1990 Stokes's formula using fast Fourier techniques. manuscripta geodaetica 15:235-239.

Torge W 1991 Geodesy (second edition), de Gruyter, Berlin.

Vaníček P, Kleusberg A 1987 The Canadian geoid — Stokesian approach. manuscripta geodaetica 12:86-98.

Vaníček P, Sjöberg LE 1991 Reformulation of Stokes's theory for higher than second-degree reference field and modification of integration kernels. Journal of Geophysical Research 96(B4):6529-6539.

Vaníček P, Featherstone WE 1998 Performance of three types of Stokes's kernel in the combined solution for the geoid. Journal of Geodesy 72(11): 684-697.

Vincent S, Marsh JG 1973 Global detailed gravimetric geoid. in: Vies (ed) Proceedings of the International Symposium on the use of Artificial Earth Satellites for Geodesy and Geodynamics, Athens, Greece, 825-855.

Wenzel H-G 1982 Geoid computation by least squares spectral combination using integral

kernels, Proceedeings of the International Association of Geodesy General Meeting, Tokyo, Japan, 438-453.

Wessel P, Smith WHF 1995 New version of the Generic Mapping Tools released, EOS - Transactions of the American Geophysical Union, 76:329.

Wichiencharoen C 1981 The indirect effects on the computation of geoid undulations. OSU Report 336, Department of Geodetic Science and Surveying, Ohio State University, Columbus USA.

Wong L, Gore R 1969 Accuracy of geoid heights from modified Stokes kernels. Geophysical Journal of the Royal Astronomical Society 18:81-91.

Zhang K 1998 A comparison of FFT geoid computation techniques and their application to GPS heighting in Australia, PhD thesis, School of Spatial Sciences, Curtin University of Technology, Perth.